LIGO SURF Final Report: Early Warning Detection of Gravitational Waves from Compact Binaries

Mariel Freyre

April 21, 2014

1 Purpose Statement

The General Theory of Relativity predicts that space and time can curve. Gravity is a geometric property of spacetime, and the forces due to gravity are really just forces due to the curvature of space. On and directly around Earth, this curvature remains in a fairly regular state, and the gravitational pull we experience as beings on this planet remains relatively constant. However, tiny fluctuations evidence themselves in the presence of ocean tides, which exist as a result of changing gravity from the Sun and the Moon. The gravitational force here is simply the curvature of spacetime, so the variations in the gravitational pull are really variations in the geometry of space and time. General relativity predicts that these variations can travel through space like a wave across a body of water. These traveling fluctuations are known as gravitational waves. [9]

Gravitational waves are the result of the motions of masses in space. A single isolated mass cannot move back and forth in space without breaking the law of conservation of momentum, but two masses in orbit around each other will "stir" spacetime enough to emit gravitational waves. [9] [7].

The technical way to think about the source of gravitational waves is a change in mass quadropoles.

Astrophysical phenomena has typically been observed using radiation from the electromagnetic spectrum. However, the field of Gravitational Wave (GW) physics has offered a new way to understand and examine the universe. Because GWs are a result of changing mass quadrupoles, the characteristics of GWs convey information about the bulk movements of matter in astrophysical systems. Electromagnetic (EM) radiation typically is emitted by the movement of charges, and therefore provide information about separate particles and not the greater structure of a system. Another important distinction between GWs and EM radiation is the fact that GWs are weakly coupled to matter. The radiation is not attenuated or scattered like photons, and theoretically should allow astronomers to observe the universe in a way that EM astronomers cannot. [8].

The most important example of a system that radiates gravitational waves is a pair of two massive objects of approximately equal mass orbiting each other circularly. The dipole moment will be constant, so the origin can be established directly between the two masses. This placement of the origin will actually cause the dipole moment to be zero, and the quadrupole moment of the system will be

$$Q_{ij} = M(3x_i x_j - \delta_{ij}) \tag{1}$$

M is the mass of each point, x_i and x_j are the components of the position vectors, and δ_{ij} is the Kronecker delta. As the masses rotate, the x vector will change in time. Therefore, the system radiates gravitational waves and loses energy in this way. This example refers to what is called a compact binary. The structure is composed of two stars, hence the word "binary," and either star must be a White Dwarf, Black Hole, or Neutron Star. The binary can be any permutation of the three types of star. These stars are *compact* and have a very intense gravity, and therefore emit distinguishable gravitational waves. [11].

The formation of compact binaries is the consequence of a chance encounter between two compact stars. The proximity of one element in the binary to another results in the emissions of gravitational waves, and thus energy. The stars would eventually lose enough energy so that they must come together and merge with each other. This process is known as compact binary coalescence (CBC). [9]

Quickly detecting CBC using early warning detectors will allow multi-messenger astronomy to observe the onset of electromagnetic emission from CBC, and by utilizing existing technology we could produce early warning triggers before gravitational radiation from the final merger has arrived at the detectors [3].

Early warning detection of GW will yield information about astrophysical phenomena even before information gathered from devices that read the electromagnetic spectrum can be collected. More importantly, this kind of detection will make it possible to change the state of an instrument in response to the presence of a signal, optimizing the sensitivity of the instrument and thus the value of the information.

The project I have worked on this summer involved implementing steps that will assist in making early detection of GWs possible. Observing gravitational waves will create a chance to understand the universe in a way that mere astronomical observation cannot. This is a huge paradigm shift: early GW detection, as a new way of observing the world, could lead to new insights regarding the nature of the universe that were previously overlooked simply because we were unable to fathom the existence of such postulates.

2 Background

Two principle properties we will be examining are the chirp mass and chirp time of a binary. The information we are able to detect from binaries reaches us in the form of a harmonic combined wave [6] . These are the gravitational waves, and they hold information regarding large scale properties of the emission process [6] [2].

When objects, such as neutron stars, orbit each other, they emit gravitational waves and as a consequence, experience a constant loss of energy. This loss of energy draws the stars closer together, resulting in a shorter orbital period and also higher frequencies of gravitational waves.

The neutron stars gain speed as they come closer together, and as they accelerate toward each other, their production of gravitational waves increases. Producing gravitational waves decreases their energy and draws them ever closer. This is something of a "vicious cycle, and it ends at the merging of the stars.

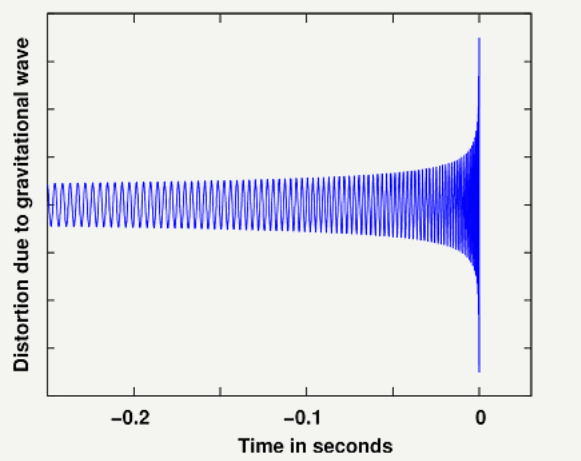

Figure 1: A "chirp" of gravitational wave data [5]

The timescale of a chirp for any binary system with stars of equal masses is in equation (2).

$$t_{chirp} = \frac{Mv^2}{2}/L_{binary} \backsim \frac{5m}{8}(\frac{M}{R})^{-4} \tag{2}$$

Early warning detection depends on how well a machine can detect the chirp mass of an object.

The instantaneous frequency of a GW inspiral is expressed as

$$f(t) = \frac{1}{\pi M_t}\left(\frac{5}{256}\frac{M_t}{t}\right)^{3/8} \quad (3)$$

$$M_c = M^{2/5}\mu^{3/5} \quad (4)$$

$$M_t = GM_c/c^3 \quad (5)$$

where M_c is the chirp mass, M_t is the chirp mass in units of time, M is the total mass, and μ is the reduced mass. [3]

An important element of the data collection process is recognizing the information given to us by the signal-to-noise ratio (SNR). Before the GW signal departs from the detection band, the SNR may already have a significant value. If this is the case, we can release an alert right away that will allow for pre-merger detection instead of S/N and sky localization accuracy. [3]

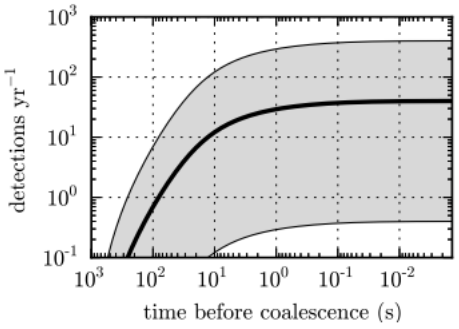

Figure 2: Expected number of NS - NS sources that could be detectable by Advanced LIGO a given number of seconds before coalescence. The heavy solid line corresponds to the most probable yearly rate estimate from Abadie et al. (2010b). The shaded region represents the 5% - 95% condence interval arising from substantial uncertainty in predicted event rates. [3]

Quantum noise originates from the physical fact that there is a finite number of photons. The position of the mirror is detected with light, but due to the discrete particle nature of light, this position is not known with total certainty, a problem introduced to us in Heisenbergs theory of uncertainty. Quantum noise in the detector has two sources. The first source is shot noise, or photon counting noise. In any finite interval, there is some uncertainty in the number of photons that will hit the mirror. The arrival of any given photon is unrelated to the arrival of any other given photon, and is thus described by a poisson distribution. The uncertainty in this distribution is the square root of the number of photons that hit the mirror. Because fractional uncertainty decreases as the number of photons increases, one way to combat shot noise is by increasing the light power of the laser in the interferometer.The small amount of absorption on the face of the optic cause thermal gradients that deform the optic and create a 'thermal lens.' The lensing effects cause the interferometer control systems to become unstable. Furthermore, an increase in light power leads to an increase in radiation pressure noise. Because the photons are randomly hitting the mirror, the mirror is pushed around by a fluctuating force that registers as a kind of stochastic noise in the data. Increasing the number of photons decreases shot noise but increases radiation pressure noise, and vice versa.

We can change the way the noise is registered by using squeezed light. Looking at the design of LIGO, we can trace the fluctuations detected at the photodetector to the photo detector– that is, there are fluctuations in the the electromagnetic field due to vacuum fluctuations. From quantum mechanics, we know that the ground state of quantum harmonic oscillator still has a modicum of energy, so nothing is ever truly still. Even the ground state of a vacuum still involves some finite amount of fluctuations, and this is responsible for the quantum noise.

3 Work Completed

Historically, when gathering data from the Laser Interferometer Gravitational Oservatory, the detector would be turned on for a certain amount of time dedicated to recording information. After this data was collected, analysts would evaluate and document whatever was relevant. However, the general behavior of a chirp sweeping across the band is fairly well known. This is the general equation describing the motion of a chirp as it sweeps across the band:

$$f(t) = \frac{1}{\pi \mathcal{M}_t} \left[\frac{5}{256} \frac{\mathcal{M}_t}{t} \right]^{3/8} \tag{6}$$

The inspiral begins at a low frequency, and as the binary looses orbital energy to gravitational waves, this frequency becomes higher and higher as the masses are drawn ever closer to each other. This behavior is described by the above equation.

Multiple sources contribute to three main sources of noise: seismic noise, thermal noise and quantum noise. At every frequency, there is a certain amount of noise power. Figure (3) displays the frequency noise. When the signal is below the noise curve, it may be indistinguishable from noise itself, thus it is negligible and impossible to observe.

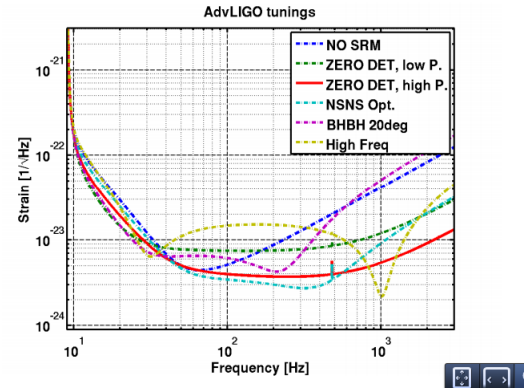

Figure 3: Anticipated noise curves of Advanced LIGO detector.

The scope of this work is to determine, given information about the first few cycles of an inspiral, whether it is possible to map out what the future frequency of the inspiral is and use that information to adjust squeeze angle to minimize quantum noise.

Suppose there is an observable random variable X. Given the Fisher matrix, we can measure the information this random variable could reveal about an unknown parameter θ when the likelihood of X depends on θ. Essentially, we are able to use the Fisher matrix formalism to determine the accuracy of parameter estimation in the measurements of gravitational wave physics.

The Fisher matrix encodes the Gaussian uncertainties of multiple variables [1]. The inverse of the Fisher matrix tells us the covariance of this data, and we can generate ellipses using this inverse, called the covariance matrix. The covariance matrix is a lower bound for the error covariance of any unbiased estimator of the true source parameters. [10] This is the Cramer-Rao bound, which is a lower bound on the variance of the estimators of a deterministic parameter. [4] the unbiased estimator that acieves this lower bound is said to be fully efficient, by which we mean that it has the minimum variance, or lowest possible mean squared error among all unbiased methods. [4].

LIGO detectors experience Gaussian noise on short time frames. With this assumption of a Gaussian distribution, we know that the covariants of our parameter θ are represented by the inverse of the Fisher matrix. We can express each element of the Fisher matrix as an inner product, shown in expression (7).

$$\mathcal{F}_{j,k} = \int_0^\infty Re \left[\left(\frac{\partial h}{\partial \theta_j} \right)^* \left(\frac{\partial h}{\partial \theta_k} \right) \right] \frac{d\omega}{S(\omega)} \tag{7}$$

The above expression can also be written:

$$\langle \frac{\partial h}{\partial \theta_j} | \frac{\partial h}{\partial \theta_k} \rangle \tag{8}$$

Following a post-newtonian expansion signal model, the variables composing the Fisher matrix are γ, which corresponds to the phase of the waveform h, τ, the time of coalescence, $\mathcal{M}_c$, the chirp mass, ω, the angular momentum, and A, the distance to the CBC. We defined the following variables :

$$\sigma^2 = \int_0^\infty \frac{|h_0|^2}{S(\omega)} d\omega \tag{9}$$

$$\rho = A\sigma \tag{10}$$

$$\overline{\omega^n} = \left(\int_0^\infty \frac{|h_0|^2}{S(\omega)} \omega^n d\omega \right) \frac{1}{\sigma^2} \tag{11}$$

We also utilize the function $h(\omega)$, which is the waveform of the signal reaching the detector. This waveform includes noise and any potential GW signal.

The matrix is displayed Fig.(4).

$$\begin{pmatrix} 1 & 0 & 0 & \frac{5\rho^2}{6\,\mathcal{M}c} \\ 0 & \rho^2 & -\rho^2\,\overline{\omega} & \frac{5\rho^2\left(G\frac{\mathcal{M}c}{2c^3}\right)^{-5/3}\overline{\omega^{-5/3}}}{128\,\mathcal{M}c} \\ 0 & -\rho^2\,\overline{\omega} & \rho^2\,\overline{\omega\hat{}2} & \frac{-\rho^2 5}{128\,\mathcal{M}c}\left(G\frac{\mathcal{M}c}{2c^3}\right)^{-5/3}\overline{\omega^{-2/3}} \\ \frac{5\rho^2}{6\,\mathcal{M}c} & \frac{5\rho^2\left(G\frac{\mathcal{M}c}{2c^3}\right)^{-5/3}\overline{\omega^{-5/3}}}{128\,\mathcal{M}c} & \frac{-\rho^2 5}{128\,\mathcal{M}c}\left(G\frac{\mathcal{M}c}{2c^3}\right)^{-5/3}\overline{\omega^{-2/3}} & \frac{25\rho^2}{36\,\mathcal{M}c^2}+\frac{\rho^2\overline{\omega^{-10/3}}25}{16\,384}\left(\frac{G\mathcal{M}c}{2c^3}\right)^{-10/3} \end{pmatrix}$$

Figure 4: This is a symmetrical matrix. Each column corresponds to a certain variable. From left to right, the order of the variables is: $\rho, \gamma, \tau, \mathcal{M}_\tau$.

In the ellipses of (5), (6) and (7), the every variable except $\mathcal{M}_\tau$ and τ were fixed.

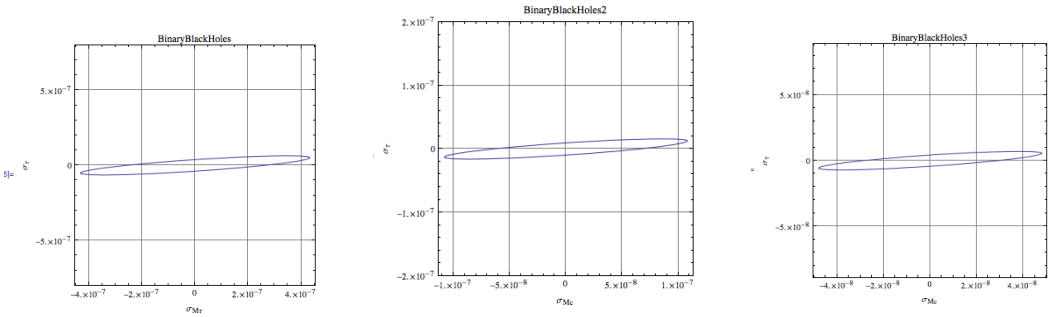

(a) SNR: $\rho = 5$ (b) SNR: $\rho = 10$ (c) SNR: $\rho = 15$.

Figure 5: Black Hole Binaries

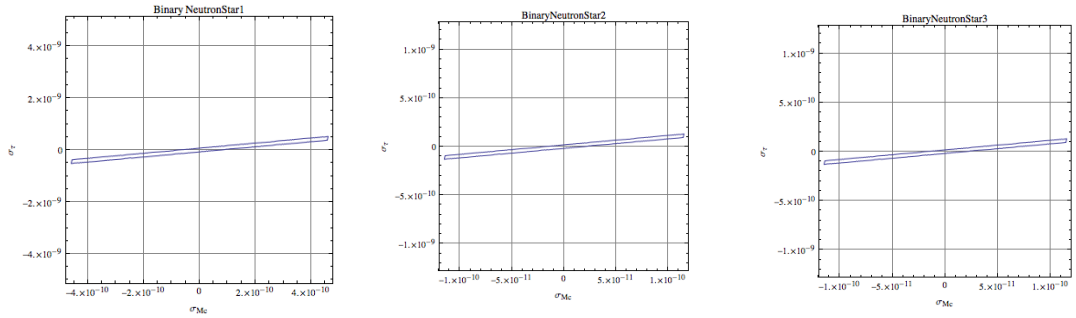

(a) SNR: $\rho = 5$ (b) SNR: $\rho = 10$ (c) SNR: $\rho = 15$.

Figure 6: Neutron star binaries

After analytically evaluating the fisher matrix, data was used to numerically evaluate the fisher matrix with code from lal and lalsimulation. The variables we observed in the numerical code were $tau_0, theta_0, theta_3, theta_{3s}$, and phi_0. The ellipses generated by the covariance matrix are below in figure (**??**).

The next step of the project was to develop plots created from theoretical Power Spectral Density (PSD) and SNR data. Using this data, I plotted the SNR vs time to coalescence for four different SNRs: SNR collected using a squeezing schedule optimized for a binary neutron star, SNR collected without a squeezing angle, SNR collected using a filter cavity, and SNR collected with a fixed squeezing angle of 7 degrees. This plot is displayed in figure (**??**). In this figure, we can see how effective optimizing the squeeze angle would be for producing the best SNR.

Given how clearly useful an optimized squeeze schedule would be in maximizing SNR, the next question to answer is, how effective will this squeeze schedule be for chirp masses that deviate from the chirp mass of a binary neutron star. In order to determine the usefulness of a binary neutron star squeeze schedule, we created a $\Delta\rho$ value that represented the difference between the optimized SNR and the unsqueezed SNR we expect from a range of masses. As the chirp mass grew larger and larger, it became clear that SNR can be lost for chirp masses of a certain large value. At this point, $\Delta\rho$ becomes negative, as we see in the following plot. Larger chirp masses are shown in red, where as smaller chirp masses are blue colored.

If an optimized squeeze schedule is extremely effective in bolstering the signal to noise ratio of a coalescing binary, it is possible that it obviates any urgent need for a filter cavity, a device which promises to be astronomically expensive while accomplishing the same goal as the squeeze schedule, a significantly less expensive endeavor. We reassigned $\Delta\rho$ to represent the difference between the optimized SNR of a binary neutron star and the SNR of data collected using a filter cavity. The value of $\Delta\rho$ appears to be smaller for chirp masses that are near the chirp mass of a binary neutron star, but $\Delta\rho$ increases significantly as the chirp mass of the filter cavity data's binary system deviates from

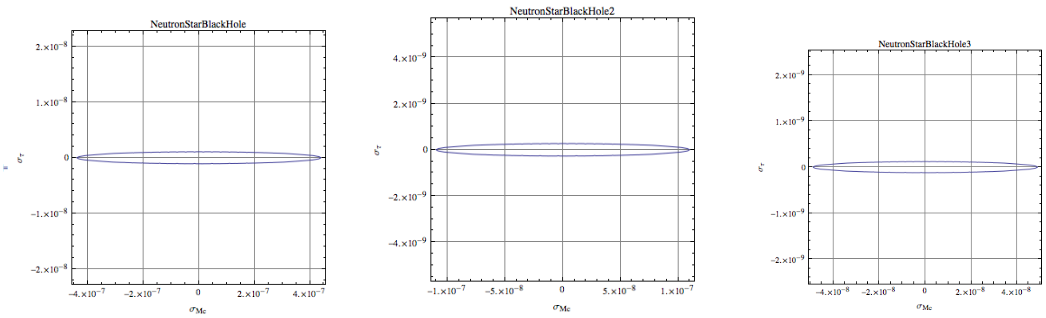

(a) SNR: $\rho = 5$ (b) SNR: $\rho = 10$ (c) SNR: $\rho = 15$

Figure 7: Black Hole Neutron Star Pairs

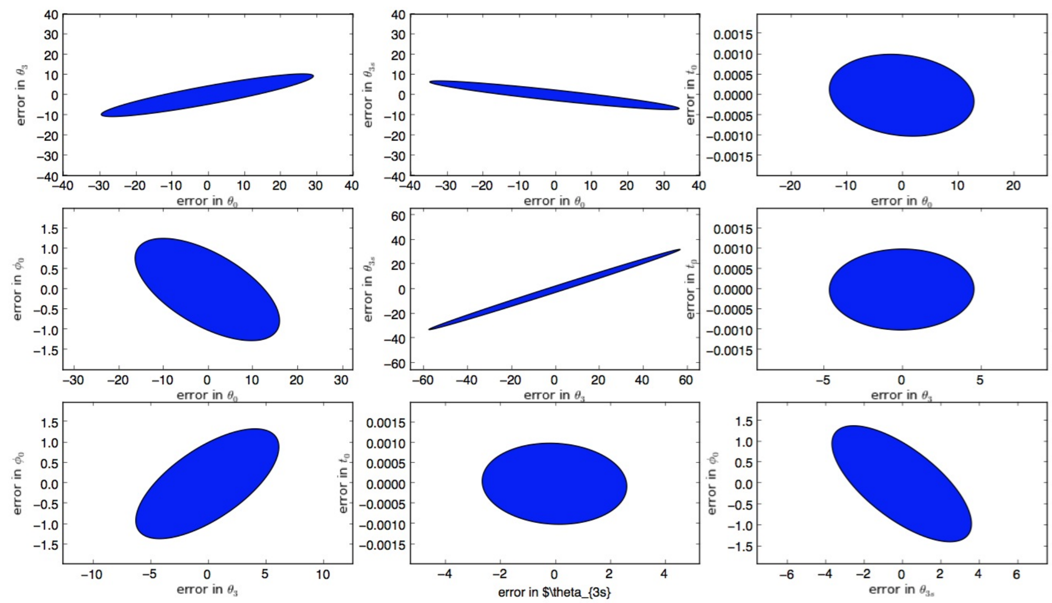

Figure 8: Numerical Ellipses

the chirp mass of the binary neutron star.

Finally, I created a script that generates colored gaussian noise and injects a waveform into this noise. The waveform is impossible to detect with the visible eye within the noise, so the script fed this data into a function that applied the FINDCHIRP algorithm in an effort to extract the relevant information from the data. The eventual goal was to develop a feedback loop from the data that adjusted the squeeze angle of the LIGO detector in order to maximize detector sensitivity, and maximize the accumulation of SNR for the coalescing binary.

4 Conclusion

While I was unable to complete a script that would adjust the LIGO detector as it collected data, I was able to show, using synthesized data, that adjusting the squeeze angle of the device in real time was an adequate substitute to implementing and installing a broadband filter cavity.

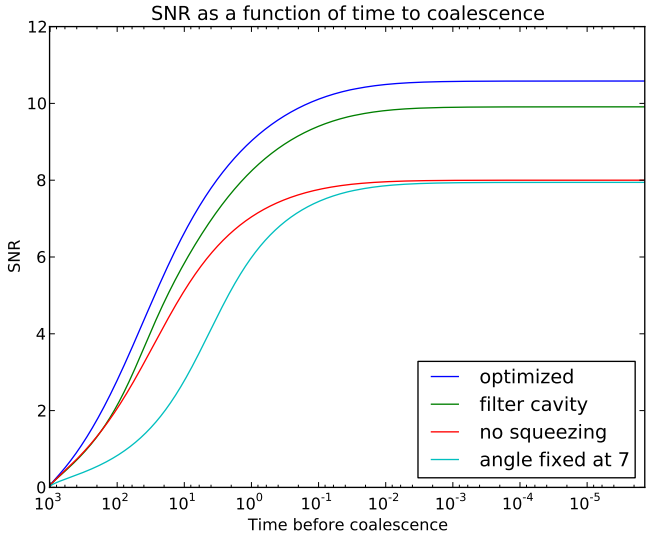

Figure 9: $\Delta\rho$ vs Time to coalescence

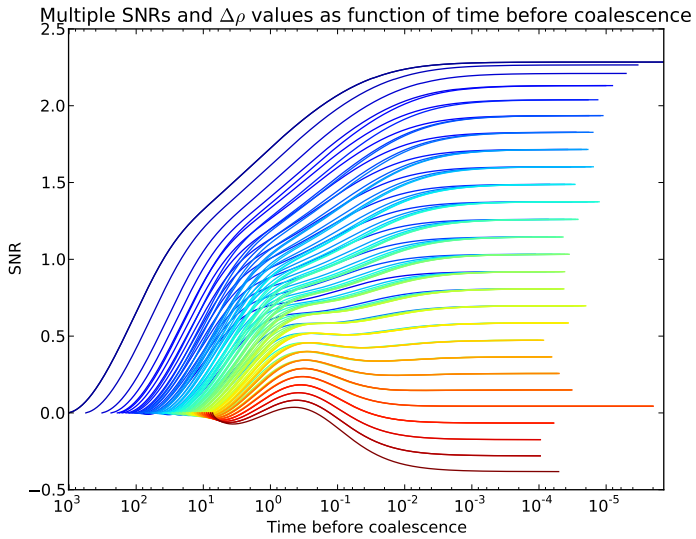

Figure 10: $\Delta\rho$ vs Time to coalescence

References

[1] Dan Coe. Fisher matrices and confidence ellipses: A quick start guide and software. 2006.

[2] Cutter Coryell. The role of small robotic telescopes in multimessenger astronomy with advanced gravitational wave detectors. 2011.

[3] Adrian Chapman Mireia Crispin-Ortuzar Leo Singer Kipp Cannon, Romain Cariou. Toward early-warning detection of gravitational waves from compact binary coalescence. 2012.

[4] David Nicholson and Alberto Vecchio. Bayesian bounds on parameter estimation accuracy for compact coalescing binary gravitational wave signals. 2008.

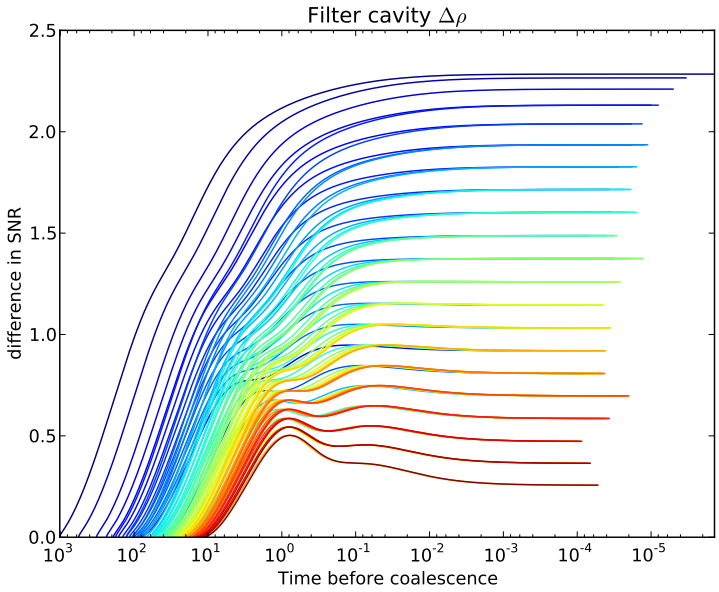

Figure 11: $\Delta\rho$ vs Time to coalescence

[5] Markus Possel. These images are available open source at
$http://www.einstein-online.info/spotlights/chirping_neutron_stars$.

[6] Markus Possel. Chirping neutron stars. *Einstein Online*, **Vol. 1**, 2005. This information is available open source at
$http://www.einstein-online.info/spotlights/chirping_neutron_stars$.

[7] Bernard F. Schultz. Gravitational wave astronomy. 1999.

[8] Bernard F. Schultz and Franco Ricci. *Gravitational Waves, Sources and Detectors*. 2010.

[9] Micheal Scott. Gravitational waves. 2011.

[10] Michele Vallisneri. A user manual for the fisher information matrix. 2007.

[11] Wikipedia. Gstreamer. 2013.